Nonlinear Analysis: Modelling and Control, Vol. 31, No. 3, 496–518
https://doi.org/10.15388/namc.2026.31.45743

Vilnius University Press

Exponential synchronization of quaternion-valued switching neural networks with mixed delays*

Wei Tan, Yongxiang Zhao[1], Tao Peng, Zhengwen Tu, Yuan Dong

School of Mathematics and Statistics,
Chongqing Three Gorges University,
Chongqing 404100, China
20100048@sanxiau.edu.cn

Received: July 3, 2025 / **Revised:** October 22, 2025 / **Published online:** March 2, 2026

Abstract. This paper investigates the exponential synchronization problem for a class of quaternion-valued switching neural networks (QVSNNs) with mixed time delays and sampled-data control. By using a Lyapunov function method involving sampling instants, sufficient conditions for the synchronization of the considered neural networks (NNs) are obtained in the form of linear matrix inequalities (LMIs). It is worth emphasizing that this paper reduces the conservativeness of stability criteria by combining the free-weight matrix method with discrete sampling points; moreover, the derived criteria are valid for both quaternion-valued and nonasynchronous switching NNs. Finally, the feasibility of the proposed approach is verified by two numerical examples.

Keywords: quaternion-valued switching neural networks, mixed delay, LMIs, sampled-data control.

1 Introduction

Quaternions, a high-dimensional mathematical system naturally extended from real and complex numbers, have one real component and three mutually orthogonal imaginary components. With the development of deep learning, researchers have explored integrating quaternions with NNs [24]. Early studies focused on quaternions' algebraic properties (e.g., noncommutativity [8]). In recent years, quaternion-valued neural networks (QVNNs) have shown great application potential in complex scenarios (e.g., satellite attitude 3D rotational modeling [4], robot multi-joint collaborative motion control [29])

*This work was jointly supported by Chongqing Municipal Natural Science Foundation Innovation Development Joint Fund (No. CSTB2023NSCQ-LZX0133), the Science and Technology Research Program of Chongqing Municipal Education Commission (Nos. KJZD-K202201202, KJZD-M202001201), the Rural Revitalization Special Project of Chongqing Science and Technology Bureau (No. CSTB2023TIAD-ZXX0017), the Foundation of Intelligent Ecotourism Subject Group of Chongqing Three Gorges University (Nos. zhlv20221001, zhlv20221029), and the Natural Science Foundation Project of Chongqing, China, under grant No. CSTB2022NSCQ-MSX0393.

[1]Corresponding author.

thanks to their high-dimensional spatial representation; these applications have significantly boosted multi-dimensional data processing and dynamic system optimization efficiency, linked to QVNNs' dynamic properties. Currently, two methods handle quaternions: decomposition and nondecomposition [11]. Decomposition was used to analyze QVNN synchronization [8, 16, 19]—though it allows direct use of real-valued NN synchronization tools to address quaternion noncommutativity, it causes a fourfold inflation of state dimensions. In contrast, nondecomposition preserves the quaternion structure and simplifies controller design [14, 22]. Consequently, this paper employs the nondecomposition approach to handle quaternions.

In the dynamic modeling of neural networks, time-varying delays in signal transmission are commonly encountered, stemming from the noninstantaneous nature of neuronal synaptic transmission [1]. This delay is not only a key driver of neural network dynamic behaviors (i.e., oscillatory modes, chaotic attractors) [6], but also directly affects the system's Lyapunov exponent synchronization. Therefore, when constructing neural network synchronization criteria, quantitative characterization of time-varying delays is key to ensuring the system's robustness [28]. In recent years, the synchronization problem of QVNNs with discrete time delays has been discussed using the decomposition method [16, 19]; the exponential stability of impulsive quaternion-valued neural networks (IQVNNs) with time delays has been studied in [20]; the sampling synchronization control of QVNNs with distributional time delays has been researched in [19,21]; the problem of mixed discrete time delays has been discussed in [25]; the combination of discrete delays and distributional delays has been explored in [2, 13, 16, 23]; the neutral-type distributed time delays have been studied using the two-sided looped functional approach [18]. Based on the above discussion, the dual action mechanisms of discrete time delays and distributed time delays are integrated in this study, and this coupled modeling approach expands the applicable scenarios of the model.

Switching systems are composed of subsystems and switching logic. Once switching rules are determined, subsystems are activated according to a predetermined sequence and dominate system evolution [30]. Existing approaches can be grouped into two categories: time-dependent switching and state-dependent switching. The former switches according to a preset cycle, and the latter switches based on state variable thresholds. In real life, it is widely used in various fields, such as UAV formation, robot collaboration [12], image encryption [27], intelligent transportation systems, and telemedicine robots [15]. The sampling control of the switching system under average dwell time (ADT) has been discussed in [3]. The synchronization of switching neural networks (SNNs) with discrete time delays has been explored in [9, 26]. The synchronization of the hybrid switching impulsive network has been discussed through designing a dual-gain saturation controller [5]. The asynchronous phenomenon of subsystem switching unsynchronized with sampling has been discussed by developing multi-Lyapunov generalized functions [10]. Some switching methods for synchronization of NNs have been discussed in [7]. The synchronization criterion for SNNs has been discussed from various aspects in previous results, but the asynchronous case under sampling control is less explored. Thus, this paper provides a more comprehensive synchronization criterion by considering both sampling-controlled synchronization and asynchrony.

Fewer studies have been conducted on the synchronization analysis of QVSNNs. However, the existing QVNNs cannot handle mode switching, and SNNs have difficulty in modeling high-dimensional data. These issues make QVSNNs a key model for solving synchronization problems in high-dimensional dynamic systems. The high-dimensional characterization ability of quaternions is integrated with the dynamic regulation mechanism of SNNs, and mixed time delays are introduced. Thus, the dimensional limitation of traditional NNs in spatio-temporal information processing can be broken through. Based on reflections on existing discussions, this paper is dedicated to establishing sufficient conditions for exponential synchronization of a class of QVSNNs with asynchronous switching and mixed time delays. The main contributions are summarized as follows:

(i) The combination of quaternions and switched neural networks has been scarcely explored in existing literature. Therefore, this paper integrates quaternions with switched neural networks to investigate their exponential synchronization.

(ii) A Lyapunov functional involving time-varying sampling intervals is proposed, combined with the free-weight matrix method at discrete sampling points. By constructing a coupling equation of sampling states and error derivatives, the conservativeness of stability criteria is reduced.

(iii) The obtained exponential synchronization criteria exhibit a broader applicability, being valid for both quaternion-valued neural networks and nonasynchronous switching neural networks.

The rest of the content is arranged as follows. Section 2 introduces the studied system and presents basic assumptions, formal definitions, and core lemmas. Section 3 proposes key theorems and proves them via rigorous theoretical derivations. Section 4 verifies the theoretical analysis through numerical simulations. Finally, Section 5 concludes.

Notations. Let r (reals), i, j, k (complexes), and $\mathbb{Q}$ (quaternions) denote the respective number systems. The matrix spaces $\mathbb{R}^{n\times n}$, $\mathbb{C}^{n\times n}$, and $\mathbb{Q}^{n\times n}$ consist of all $n\times n$ matrices over $\mathbb{R}$, $\mathbb{C}$, and $\mathbb{Q}$, correspondingly. We write $\mathbb{R}^n$ (resp. $\mathbb{C}^n$, $\mathbb{Q}^n$) for the space of n-dimensional real (resp. complex, quaternion) vectors. Let A^{T} be the transpose, $\bar{A}$ the conjugate, and $A^* = \bar{A}^{\mathrm{T}}$ the conjugate transpose of matrix A. For any $A \in \mathbb{Q}^{n\times n}$, the module of A is denoted by $|A|$, while $\|A\|$ indicates its norm, $\lambda_{\min}(A)$ and $\lambda_{\max}(A)$ correspond to the minimum and maximum eigenvalues, respectively.

2 Preliminaries

2.1 Model description

Consider the dynamic behavior of QVSNN with discrete and distributed time-varying delays under the action of switching signal, which is described by the following model:

$$\begin{aligned}\dot{x}(t) = {} & -A_{\sigma(t)}x(t) + B_{\sigma(t)}f\big(x(t)\big) + C_{\sigma(t)}f\big(x\big(t-d(t)\big)\big) \\ & + D_{\sigma(t)}\int_{t-\tau(t)}^{t} f\big(x(s)\big)\,\mathrm{d}s + I(t),\end{aligned} \tag{1}$$

where $x(t) = (x_1(t), x_2(t), \dots, x_n(t))^{\mathrm{T}} \in \mathbb{Q}^n$ is the state vector of the neuron, $f(\cdot) = (f_1(\cdot), f_2(\cdot), \dots, f_n(\cdot))^{\mathrm{T}} \in \mathbb{Q}^n$ is the activation function of the neuron, $\sigma(t)\colon[t_0, \infty) \to \mathbb{M} = \{1, 2, \dots, n, \dots\}$ is the switching signal. $A_{\sigma(t)} \in \mathbb{R}^{n\times n}$ is a positive definite diagonal matrix, $B_{\sigma(t)} = (b_{ij})_{n\times n}$, $C_{\sigma(t)} = (c_{ij})_{n\times n}$ and $D_{\sigma(t)} = (d_{ij})_{n\times n} \in \mathbb{Q}^{n\times n}$ are connection weight matrices. $I(t) = (I_1(t), I_2(t), \dots I_n(t))^{\mathrm{T}} \in \mathbb{Q}^n$ is an external input to a neural network, $d(t)$ and $\tau(t)$ denote discrete time-varying delay and distributed time-varying delay, respectively. Moreover,

$$0 \leqslant d(t) \leqslant d, \qquad 0 \leqslant \dot{d}(t) \leqslant d_1 < 1, \qquad 0 \leqslant \tau(t) \leqslant \tau < 1.$$

Setting QVSNN (1) as the master system, we construct controlled slave systems whose switching rules are the same as those of system (1). The construction can be described as follows:

$$\begin{aligned}\dot{y}(t) = {} & -A_{\sigma(t)}y(t) + B_{\sigma(t)}f\big(y(t)\big) + C_{\sigma(t)}f\big(y\big(t - d(t)\big)\big) \\ & + D_{\sigma(t)}\int_{t-\tau(t)}^{t} f\big(y(s)\big)\,\mathrm{d}s + I(t) + U(t),\end{aligned} \tag{2}$$

where $y(t) = (y_1(t), y_2(t), \dots, y_n(t))^{\mathrm{T}} \in \mathbb{Q}^n$ is the state vector of the neuron, $U(t)$ is the controller to be designed.

By defining $r(t) = y(t) - x(t)$, $g(r(t)) = f(y(t)) - f(x(t))$, a master-slave synchronization error system can be obtained:

$$\begin{aligned}\dot{r}(t) = {} & -A_{\sigma(t)}r(t) + B_{\sigma(t)}g\big(r(t)\big) + C_{\sigma(t)}g\big(r\big(t - d(t)\big)\big) \\ & + D_{\sigma(t)}\int_{t-\tau(t)}^{t} g\big(r(s)\big)\,\mathrm{d}s + U(t).\end{aligned} \tag{3}$$

In this paper, sampled-data feedback control is used to achieve the synchronization of the network, and the control input of the system can be expressed as follows:

$$U(t) = K_{\sigma(t)}r(t_k), \quad t_k \leqslant t \leqslant t_{k+1}. \tag{4}$$

Assume that the sampling interval is time-varying and satisfies

$$0 \leqslant t_{k+1} - t_k = h_k \leqslant h,$$

where h is a constant.

Combining (3) and (4), we can obtain

$$\begin{aligned}\dot{r}(t) = {} & -A_{\sigma(t)}r(t) + B_{\sigma(t)}g\big(r(t)\big) + C_{\sigma(t)}g\big(r(t - d(t))\big) \\ & + D_{\sigma(t)}\int_{t-\tau(t)}^{t} g(r(s))\,\mathrm{d}s + K_{\sigma(t)}r(t_k).\end{aligned} \tag{5}$$

When considering asynchronous switching, let $t_k+\bar{t}$ be the switching moment, where $\bar{t} \in (0, h]$. Before the switch occurs, for $t \in [t_k, t_k + \bar{t})$, $\sigma(t) = i$, and the system and controller are matched. However, after switching, $t \in [t + \bar{t}, t_{k+1})$, $\sigma(t) = j$, and the controller remains unchanged until the next sampling moment. This results in a mismatch between the system and the controller. It can be obtained that

$$\dot{r}(t) = \begin{cases} \dot{r}_i(t), & t \in [t_k, t + \bar{t}), \\ \dot{r}_j(t), & t \in [t + \bar{t}, t_{k+1}), \end{cases} \tag{6}$$

where

$$\begin{aligned} \dot{r_i}(t) &= -A_i r(t) + B_i g\big(r(t)\big) + C_i g\big(r\big(t - d(t)\big)\big) \\ &\quad + D_i \int\limits_{t-\tau(t)}^{t} g\big(r(s)\big)\,\mathrm{d}s + K_i r(t_k), \\ \dot{r_j}(t) &= -A_j r(t) + B_j g\big(r(t)\big) + C_j g\big(r\big(t - d(t)\big)\big) \\ &\quad + D_j \int\limits_{t-\tau(t)}^{t} g\big(r(s)\big)\,\mathrm{d}s + K_i r(t_k). \end{aligned}$$

2.2 Assumption, definition, and lemma

Some assumptions needed for this paper are given below.

Assumption 1. For any $x_1, x_2 \in \mathbb{Q}$, there are scalars $L_i > 0$ such that

$$\big|f_i(x_1) - f_i(x_2)\big| \leqslant L_i|x_1 - x_2|, \quad L_i \in \mathbb{R},\ i = 1, 2, \ldots, n.$$

Here $L = \operatorname{diag}(L_1, L_2, \ldots, L_n)$.

Assumption 2. The switching signal $\sigma(t)$ has a dwell time τ_d. It is assumed that a switch occurs at most once within a sampling interval such that $h_k \leqslant \tau_d$.

The definitions needed for this paper are given below.

Definition 1. (See [23].) If the error system (3) is exponentially stable, it is said that the master-slave system (1) and (2) achieve exponential synchronization. In other words, there exist two constants λ_1, $\lambda_2 > 0$ satisfying

$$\big\|r(t)\big\| \leqslant \lambda_1 \mathrm{e}^{-\lambda_2(t-t_0)}\big\|r(t_0)\big\|, \quad t \geqslant t_0,$$

where λ_1 and λ_2 represent the decay coefficient and rate, respectively.

Definition 2. (See [3].) There exists a constant $\tau_d > 0$ (called the dwell time) such that the interval between any two switches is greater than τ_d. Moreover, suppose that there exist constants $\tau_a \geqslant \tau_d$ and $N_0 \geqslant 1$ satisfying

$$N_\sigma(T, t) \leqslant N_0 + \frac{T - t}{\tau_a}, \quad 0 \leqslant t \leqslant T,$$

where $N_\sigma(T,t)$ counts the switchings of $\sigma(t)$ over the interval (t,T); τ_a represents the average dwell time, and N_0 is the chatter bound.

The lemmas needed for this paper are given below.

Lemma 1. (*See* [17].) *Given a positive definite matrix $K \in \mathbb{Q}^{n\times n}$ (Hermitian) and a function $\vartheta(\kappa) : [a,b] \to \mathbb{Q}^n$ ($a < b$), the following inequality holds*:

$$\left(\int_a^b \vartheta(\kappa)\,\mathrm{d}\kappa\right)^* K\left(\int_a^b \vartheta(\kappa)\,\mathrm{d}\kappa\right) \leqslant (b-a)\int_a^b \vartheta^*(\kappa)K\vartheta(\kappa)\,\mathrm{d}\kappa,$$

where $\vartheta(\kappa) : [a,b] \to \mathbb{Q}^n$ is a quaternion vector-valued function, and $\vartheta^*(\kappa)$ denotes its Hermitian transpose.

Lemma 2. (*See* [20].) *Given a matrix $Q \in \mathbb{Q}^{n\times n}$ (Hermitian), then $Q \prec 0$ is equivalent to*

$$\begin{bmatrix} Q^{(r)} & -Q^{(j)} & -Q^{(i)} & Q^{(k)} \\ Q^{(j)} & Q^{(r)} & Q^{(k)} & Q^{(i)} \\ Q^{(i)} & -Q^{(k)} & Q^{(r)} & -Q^{(j)} \\ -Q^{(k)} & -Q^{(i)} & Q^{(j)} & Q^{(r)} \end{bmatrix} < 0,$$

where $Q^{(r)}, Q^{(i)}, Q^{(j)}, Q^{(k)} \in R^{n\times n}$ are real matrices formed by the real parts, coefficients of the i imaginary parts, coefficients of the j imaginary parts, and coefficients of the k imaginary parts of all elements in Q, respectively.

Lemma 3 [Wirtinger-based inequality]. (*See* [22].) *For any positive definite matrix $H \in \mathbb{Q}^{n\times n}$ (Hermitian), let the function $\zeta(\kappa) : [c,d] \to \mathbb{Q}^n$ be continuously differentiable. Then the following inequality holds*:

$$\int_c^d \dot{\zeta}^*(\kappa)H\dot{\zeta}(\kappa)\,\mathrm{d}\kappa \geqslant \frac{1}{d-c}\big(\zeta(d)-\zeta(c)\big)^* H\big(\zeta(d)-\zeta(c)\big) + \frac{3}{d-c}\aleph^* H\aleph,$$

where

$$\aleph = \zeta(d)+\zeta(c)-\frac{2}{d-c}\int_c^d \zeta(\kappa)\,\mathrm{d}\kappa.$$

3 Main results

Firstly, we consider error systems with asynchronous switching. In each sampling interval, Assumption 2 ensures no more than one switching event: if no switching occurs, the activated subsystem matches the controller; if switching occurs, the interval splits into two parts—the first where the activated subsystem matches the controller, and the second where post-switching mismatch persists until the next sampling moment, causing asynchrony between the subsystem and the controller.

Theorem 1. *Under Assumption* 1–2*, suppose that for* $\alpha, \beta > 0$ *and any* h*, there exist positive definite Hermitian matrices* $P_i, P_{ij}, Q_{1i}, Q_{1ij}, Q_{2i}, Q_{2ij}, Q_{3i}, Q_{3ij}, S_i, S_{ij}, L_i, L_j, R_{1i}, R_{1ij}, R_{2i}, R_{2ij} \in \mathbb{R}^{n\times n}$ *and any matrices* M_i*,* G_i *guaranteeing the feasibility of the LMIs*

$$\Xi_i = \begin{bmatrix} \Xi_{11i} & -A_i^*G_i^* & 0 & 0 & P_i^*B_i & P_i^*C_i & 0 & P_i^*D_i & \Xi_{19i} \\ * & \Xi_{22i} & 0 & 0 & G_iB_i & G_iC_i & 0 & G_iD_i & M_i - G_i^* \\ * & * & \Xi_{33i} & 0 & 0 & 0 & 0 & 0 & 0 \\ * & * & * & \Xi_{44i} & 0 & 0 & 0 & 0 & 0 \\ * & * & * & * & \Xi_{55i} & 0 & 0 & 0 & B_i^*G_i^* \\ * & * & * & * & * & \Xi_{66i} & 0 & 0 & C_i^*G_i^* \\ * & * & * & * & * & * & \Xi_{77i} & 0 & 0 \\ * & * & * & * & * & * & * & \Xi_{88i} & D_i^*G_i^* \\ * & * & * & * & * & * & * & * & \Xi_{99i} \end{bmatrix} \prec 0, \tag{7}$$

$$\Xi_{ij} = \begin{bmatrix} \Xi_{11ij} & -A_j^*G_i^* & 0 & 0 & P_{ij}^*B_j & P_{ij}^*C_j & 0 & P_{ij}^*D_j & \Xi_{19ij} \\ * & \Xi_{22ij} & 0 & 0 & G_iB_j & G_iC_j & 0 & G_iD_j & M_i - G_i^* \\ * & * & \Xi_{33ij} & 0 & 0 & 0 & 0 & 0 & 0 \\ * & * & * & \Xi_{44ij} & 0 & 0 & 0 & 0 & 0 \\ * & * & * & * & \Xi_{55ij} & 0 & 0 & 0 & B_j^*G_i^* \\ * & * & * & * & * & \Xi_{66ij} & 0 & 0 & C_j^*G_i^* \\ * & * & * & * & * & * & \Xi_{77ij} & 0 & 0 \\ * & * & * & * & * & * & * & \Xi_{88ij} & D_j^*G_i^* \\ * & * & * & * & * & * & * & * & \Xi_{99ij} \end{bmatrix} \prec 0,$$

where

$$\Xi_{11i} = 2\alpha P_i - A_i^*P_i - P_i^*A_i + Q_{1i} + L_i^*R_{1i}L_i - \frac{1}{h}\mathrm{e}^{-2\alpha h}S_i - \mathrm{e}^{2\alpha d}Q_{2i},$$

$$\Xi_{19i} = \frac{1}{h}\mathrm{e}^{-2\alpha h}S_i + P_iG_i^{-1}M_i - A_i^*G_i^*, \qquad \Xi_{22i} = d^2Q_{2i} + hS_i - G_i - G_i^*,$$

$$\Xi_{33i} = -(1-d_1)\mathrm{e}^{-2\alpha d}Q_{1i} + L_i^*R_{2i}L_i, \qquad \Xi_{44i} = -\mathrm{e}^{2\alpha d}Q_{2i}, \Xi_{55i} = \tau^2Q_{3i} - R_{1i},$$

$$\Xi_{66i} = -R_{2i}, \qquad \Xi_{77i} = -\mathrm{e}^{2\alpha d}\frac{1}{d}Q_{2i}, \qquad \Xi_{88i} = -\mathrm{e}^{2\alpha\tau}Q_{3i},$$

$$\Xi_{99i} = -\frac{1}{h}\mathrm{e}^{-2\alpha h}S_i + M_i + M_i^*,$$

$$\Xi_{11ij} = -2\beta P_{ij} - A_j^*P_{ij} - P_{ij}^*A_j + Q_{1ij} + L_j^*R_{1ij}L_j - \frac{1}{h}\mathrm{e}^{2\beta h}S_{ij} - \mathrm{e}^{2\beta d}Q_{2ij},$$

$$\Xi_{19ij} = \frac{1}{h}\mathrm{e}^{2\beta h}S_{ij} + P_jG_i^{-1}M_i - A_j^*G_i^*, \qquad \Xi_{22ij} = d^2Q_{2ij} + hS_{ij} - G_i - G_i^*,$$

$$\Xi_{33ij} = -(1-d_1)\mathrm{e}^{2\beta d}Q_{1ij} + L_j^*R_{2ij}L_j, \qquad \Xi_{44ij} = -\mathrm{e}^{-2\beta d}Q_{2ij},$$

$$\Xi_{55ij} = \tau^2Q_{3i} - R_{1ij}, \qquad \Xi_{66ij} = -R_{2ij}, \qquad \Xi_{77ij} = -\mathrm{e}^{-2\beta d}\frac{1}{d}Q_{2ij},$$

$$\Xi_{88ij} = -\mathrm{e}^{-2\beta\tau}Q_{3ij}, \qquad \Xi_{99ij} = -\frac{1}{h}\mathrm{e}^{2\beta h}S_{ij} + M_i + M_i^*,$$

$$\begin{aligned} &Q_{1ij} \leqslant \mathrm{e}^{-2(\alpha+\beta)d}\mu Q_{1i}, \qquad Q_{2ij} \leqslant \mathrm{e}^{-2(\alpha+\beta)d}\mu Q_{2i}, \\ &Q_{3ij} \leqslant \mathrm{e}^{-2(\alpha+\beta)\tau}\mu Q_{3i}, \qquad S_{ij} \leqslant \mathrm{e}^{-2(\alpha+\beta)h}\mu S_i, \qquad P_{ij} \leqslant \mu P_i. \end{aligned} \tag{8}$$

Then the ADT satisfies

$$\tau_a \geqslant \left(1 + \frac{\beta h + ln\mu}{\alpha h}\right)h, \tag{9}$$

and the error system (5) *with asynchronous switching can be exponentially stable through the controller given by* $K_i = G_i^{-1}M_i$.

Proof. When considering systems with asynchronous switching, we can divide the sampling intervals into two cases: one in which no switching occurs during a complete sampling interval; the other in which switching occurs once during a sampling interval.

Case 1. Sampling interval without switch.

When the ith subsystem is activated during the entire interval $[t_k, t_{k+1})$. From (6) the closed-loop dynamics is given by the following equation:

$$\begin{aligned} \dot{r}_i(t) = {} & -A_i r(t) + B_i g\big(r(t)\big) + C_i g\big(r\big(t - d(t)\big)\big) \\ & + D_i \int_{t-\tau(t)}^{t} g\big(r(s)\big)\,\mathrm{d}s + K_i r(t_k). \end{aligned} \tag{10}$$

Consider the LKF candidate as follows:

$$V_i\big(r(t)\big) = V_{1i}\big(r(t)\big) + V_{2i}\big(r(t)\big) + V_{3i}\big(r(t)\big) + V_{4i}\big(r(t)\big) + V_{5i}\big(r(t)\big), \tag{11}$$

where

$$\begin{aligned} V_{1i}\big(r(t)\big) &= r^*(t)P_i r(t), \\ V_{2i}\big(r(t)\big) &= \int_{t-d(t)}^{t} \mathrm{e}^{-2\alpha(t-s)} r^*(s) Q_{1i} r(s)\,\mathrm{d}s, \\ V_{3i}\big(r(t)\big) &= d\int_{-d}^{0}\int_{t+\theta}^{t} \mathrm{e}^{-2\alpha(t-s)} \dot{r}^*(s) Q_{2i} \dot{r}(s)\,\mathrm{d}s\,\mathrm{d}\theta, \\ V_{4i}\big(r(t)\big) &= \tau\int_{-\tau}^{0}\int_{t+\theta}^{t} \mathrm{e}^{-2\alpha(t-s)} g^*(r(s)) Q_{3i} g\big(r(s)\big)\,\mathrm{d}s\,\mathrm{d}\theta, \\ V_{5i}\big(r(t)\big) &= (t_{k+1} - t)\int_{t_k}^{t} \mathrm{e}^{-2\alpha(t-s)} \dot{r}^*(s) S_i \dot{r}(s)\,\mathrm{d}s, \quad t \in [t_k, t_{k+1}]. \end{aligned}$$

Calculating the derivative of $V_i(\mathrm{r}(t))$ along the trajectory of (10) yields

$$\begin{aligned} \dot{V}_{1i}\big(r(t)\big) &= -2\alpha V_{1i} + \dot{r}^*(t)P_i r(t) + r^*(t)P_i^* \dot{r}(t) + 2\alpha r^*(t)P_i r(t) \\ &= -2\alpha V_{1i} + 2\alpha r^*(t)P_i r(t) \end{aligned}$$

$$
\begin{aligned}
&+ r^*(t)(-A_i^*P_i)r(t) + g^*\big(r(t)\big)(B_i^*P_i)r(t)\\
&+ g^*\big(r\big(t-d(t)\big)\big)(C_i^*P_i)r(t) + \left(\int_{t-\tau(t)}^{t} g\big(r(s)\big)\,\mathrm{d}s\right)^*(D_i^*P_i)r(t)\\
&+ r^*(t_k)K_i^*P_ir(t) + r^*(t)(-P_i^*A_i)r(t) + r^*(t)(P_i^*B_i)g\big(r(t)\big)\\
&+ r^*(t)(P_i^*C_i)g\big(r\big(t-d(t)\big)\big) + r^*(t)(P_i^*D_i)\int_{t-\tau(t)}^{t} g\big(r(s)\big)\,\mathrm{d}s\\
&+ r^*(t)P_i^*K_ir(t_k), \qquad (12)
\end{aligned}
$$

$$
\begin{aligned}
\dot V_{2i}\big(r(t)\big) \leqslant{}& -2\alpha V_{2i} + r^*(t)Q_{1i}r(t)\\
&- (1-d_1)\mathrm{e}^{-2\alpha d}r^*\big(t-d(t)\big)Q_{1i}r\big(t-d(t)\big), \qquad (13)
\end{aligned}
$$

$$
\dot V_{3i}\big(r(t)\big) \leqslant -2\alpha V_{3i} + d^2\dot r^*(t)Q_{2i}\dot r(t) - d\mathrm{e}^{2\alpha d}\int_{t-d}^{t}\dot r^*(s)Q_{2i}\dot r(s)\,\mathrm{d}s, \qquad (14)
$$

$$
\dot V_{4i}\big(r(t)\big) \leqslant -2\alpha V_{4i} + \tau^2 g^*\big(r(t)\big)Q_{3i}g\big(r(t)\big) - \tau\mathrm{e}^{2\alpha\tau}\int_{t-\tau}^{t} g^*\big(r(s)\big)Q_{3i}g\big(r(s)\big)\,\mathrm{d}s,
$$

$$
\dot V_{5i}\big(r(t)\big) = -2\alpha V_{5i} - \int_{t_k}^{t}\mathrm{e}^{-2\alpha(t-s)}\dot r^*(s)S_i\dot r(s)\,\mathrm{d}s + (t_{k+1}-t)\dot r^*(t)S_i\dot r(t).
$$

The integral term in (14) can be transformed by using Lemma 3:

$$
\dot V_{3i}\big(r(t)\big) \leqslant -2\alpha V_{3i} + d^2\dot r^*(t)Q_{2i}\dot r(t) - \mathrm{e}^{2\alpha d}N_i^*Q_{2i}N_i, \qquad (15)
$$

where $N_i = [r^*(t)r^*(t-d)(1/d)\int_{t-d}^{t} r^*(s)\,\mathrm{d}s]^*$.

By using Lemma 1, we have

$$
\begin{aligned}
\dot V_{4i}\big(r(t)\big) \leqslant{}& -2\alpha V_{4i} + \tau^2 g^*\big(r(t)\big)Q_{3i}g\big(r(t)\big)\\
&- \mathrm{e}^{2\alpha\tau}\left(\int_{t-\tau}^{t} g\big(r(s)\big)\,\mathrm{d}s\right)^* Q_{3i}\left(\int_{t-\tau}^{t} g\big(r(s)\big)\,\mathrm{d}s\right). \qquad (16)
\end{aligned}
$$

By using Jensen's inequality and Newton–Leibniz formula, it follows that

$$
\begin{aligned}
\dot V_{5i}\big(r(t)\big) \leqslant{}& -2\alpha V_{5i} - \frac{1}{h}\mathrm{e}^{-2\alpha h}\big(r(t)-r(t_k)\big)^* S_i\big(r(t)-r(t_k)\big)\\
&+ h\dot r^*(t)S_i\dot r(t). \qquad (17)
\end{aligned}
$$

For any matrix G_i, the following equation holds:

$$\begin{aligned}0 ={}& \big[\dot r(t)+r(t_k)\big]^* G_i\big(-\dot r(t)-A_i r(t)+B_i g\big(r(t)\big)+C_i g\big(r\big(t-d(t)\big)\big)\big)\\ &+\big[\dot r(t)+r(t_k)\big]^* G_i\left(D_i\int_{t-\tau(t)}^{t} g\big(r(s)\big)\,\mathrm{d}s+K_i r(t_k)\right)\\ &+\big(-\dot r(t)-A_i r(t)+B_i g\big(r(t)\big)+C_i g\big(r\big(t-d(t)\big)\big)\big)^* G_i^*\big[\dot r(t)+r(t_k)\big]\\ &+\left(D_i\int_{t-\tau(t)}^{t} g\big(r(s)\big)\,\mathrm{d}s+K_i r(t_k)\right)^* G_i^*\big[\dot r(t)+r(t_k)\big]. \end{aligned}\tag{18}$$

Based on Assumption 1, we obtain the following inequalities:

$$g^*\big(r(t)\big)R_{1i}g\big(r(t)\big)\leqslant r^*(t)(L_i^*R_{1i}L_i)r(t),\tag{19}$$

$$g^*\big(r\big(t-d(t)\big)\big)R_{2i}g\big(r\big(t-d(t)\big)\big)\leqslant r^*\big(t-d(t)\big)(L_i^*R_{2i}L_i)r\big(t-d(t)\big).\tag{20}$$

Combining with (12), (13), and (15)–(20), the LKF satisfies

$$\begin{aligned}\dot V_i\big(r(t)\big)={}&\dot V_{1i}\big(r(t)\big)+\dot V_{2i}\big(r(t)\big)+\dot V_{3i}\big(r(t)\big)+\dot V_{4i}\big(r(t)\big)+\dot V_{5i}\big(r(t)\big)\\ \leqslant{}&-2\alpha V_i\big(r(t)\big)+r^*(t)(2\alpha P_i+Q_{1i}-A_i^*P_i-P_i^*A_i-\mathrm{e}^{2\alpha d}Q_{2i})\\ &+r^*(t)\left(-\frac{1}{h}\mathrm{e}^{2\alpha h}S_i+L_i^*R_{1i}L_i\right)r(t)\\ &+\dot r^*(t)\big(d^2Q_{2i}+hS_i-G_i-G_i^*\big)\dot r(t)+r^*(t-d)\big(-\mathrm{e}^{-2\alpha d}Q_{2i}\big)r(t-d)\\ &+r^*\big(t-d(t)\big)\big(-(1-d_1)\mathrm{e}^{-2\alpha d}Q_{1i}+L_i^*R_{2i}L_i\big)r\big(t-d(t)\big)\\ &+g^*\big(r(t)\big)\big(\tau^2Q_{3i}-R_{1i}\big)g\big(r(t)\big)+g^*\big(r\big(t-d(t)\big)\big)(-R_{2i})g\big(r\big(t-d(t)\big)\big)\\ &+\left(\int_{t-d}^{t} r(s)\,\mathrm{d}s\right)^*\left(-\frac{1}{d}\mathrm{e}^{2\alpha d}Q_{2i}\right)\left(\int_{t-d}^{t} r(s)\,\mathrm{d}s\right)\\ &+\left(\int_{t-\tau}^{t} g\big(r(s)\big)\,\mathrm{d}s\right)^*\big(-\mathrm{e}^{2\alpha\tau}Q_{3i}\big)\left(\int_{t-\tau}^{t} g\big(r(s)\big)\,\mathrm{d}s\right)\\ &+r^*(t_k)\left(-\frac{1}{h}\mathrm{e}^{-2\alpha h}S_i+G_iK_i+K_i^*G_i^*\right)r(t_k)+r^*(t)(-A_i^*G_i^*)\dot r(t)\\ &+r^*(t)P_i^*B_ig\big(r(t)\big)+r^*(t)P_i^*C_ig\big(r\big(t-d(t)\big)\big)\\ &+r^*(t)P_i^*D_i\int_{t-\tau}^{t} g\big(r(s)\big)\,\mathrm{d}s+r^*(t)\left(\frac{1}{h}\mathrm{e}^{-2\alpha h}S_i+P_iK_i\right)r(t_k)\\ &+\dot r^*(t)(-G_iA_i)r(t)+\dot r^*(t)G_iB_ig\big(r(t)\big)+\dot r^*(t)G_iC_ig\big(r\big(t-d(t)\big)\big)\end{aligned}$$

$$
\begin{aligned}
&+ \dot{r}^*(t)G_iD_i\int_{t-\tau}^{t} g\big(r(s)\big)\,\mathrm{d}s + \dot{r}^*(t)G_iK_ir(t_k) + g^*\big(r(t)\big)B_i^*P_ir(t)\\
&+ g^*\big(r(t)\big)B_i^*G_i^*\dot{r}(t) + g^*\big(r(t)\big)B_i^*G_i^*r(t_k) + g^*\big(r\big(t-d(t)\big)\big)C_i^*P_ir(t)\\
&+ g^*\big(r\big(t-d(t)\big)\big)C_i^*G_i^*\dot{r}(t) + g^*\big(r\big(t-d(t)\big)\big)C_i^*G_i^*r(t_k)\\
&+ \left(\int_{t-\tau}^{t} g\big(r(s)\big)\,\mathrm{d}s\right)^*D_i^*P_ir(t) + \left(\int_{t-\tau}^{t} g\big(r(s)\big)\,\mathrm{d}s\right)^*D_i^*G_i^*\dot{r}(t)\\
&+ \left(\int_{t-\tau}^{t} g\big(r(s)\big)\,\mathrm{d}s\right)^*D_i^*G_i^*r(t_k) + r^*(t_k)\left(\frac{1}{h}\mathrm{e}^{-2\alpha h}S_i + K_i^*P_i\right)r(t)\\
&+ r^*(t_k)K_i^*G_i^*\dot{r}(t) + r^*(t_k)G_iB_ig\big(r(t)\big)\\
&+ r^*(t_k)G_iC_ig\big(r\big(t-d(t)\big)\big) + r^*(t_k)G_iD_i\int_{t-\tau}^{t} g\big(r(s)\big)\,\mathrm{d}s\\
\leqslant\ & -2\alpha V_i\big(r(t)\big) + \Phi^*(t)\Xi_i\Phi(t),
\end{aligned}
$$

where

$$
\begin{aligned}
\Phi(t) = \Bigg[& r^*(t),\ \dot{r}^*(t),\ r^*\big(t-d(t)\big),\ r^*(t-d),\ g^*\big(r(t)\big),\ g^*\big(r\big(t-d(t)\big)\big),\\
&\left(\int_{t-d}^{t} r(s)\,\mathrm{d}s\right)^*,\ \left(\int_{t-\tau}^{t} g\big(r(s)\big)\,\mathrm{d}s\right)^*,\ r^*(t_k)\Bigg]^*.
\end{aligned}
$$

From (7) we can obtain

$$
\dot{V}_i\big(r(t)\big) < -2\alpha V_i\big(r(t)\big). \tag{21}
$$

For $t \in [t_k, t_{k+1}]$, integrating (21) yields

$$
V_i\big(r(t_{k+1})\big) < \mathrm{e}^{-2\alpha(t_{k+1}-t_k)}V_i\big(r(t_k)\big). \tag{22}
$$

Case 2. Sampling interval with one switch.

In this case, two subsystems will exist within the interval $[t_k, t_{k+1})$, namely $\sigma_{t_k} = i$ and $\sigma_{t_{k+1}} = j \neq i$. The controller can get the system switching information only at the sampling time. From (6) if $t \in (t_k,\ t_k + \bar{t}]$, the ith subsystem will be activated. Similar to Case 1, it can be derived that

$$
V_i\big(r(t)\big) < \mathrm{e}^{-2\alpha(t-t_k)}V_i\big(r(t_k)\big). \tag{23}
$$

When $t \in (t_k + \bar{t},\, t_{k+1}]$, the closed-loop dynamic becomes

$$\begin{aligned}\dot{r}_j(t) = {} & -A_j r(t) + B_j g\big(r(t)\big) + C_j g\big(r\big(t - d(t)\big)\big) \\ & + D_j \int_{t-\tau(t)}^{t} g\big(r(s)\big)\,\mathrm{d}s + K_i r(t_k).\end{aligned} \tag{24}$$

Consider the LKF candidate as follows:

$$V_{ij}\big(r(t)\big) = V_{1ij}\big(r(t)\big) + V_{2ij}\big(r(t)\big) + V_{3ij}\big(r(t)\big) + V_{4ij}\big(r(t)\big) + V_{5ij}\big(r(t)\big), \tag{25}$$

where

$$\begin{aligned}V_{1ij}\big(r(t)\big) &= r^*(t) P_{ij} r(t), \\ V_{2ij}\big(r(t)\big) &= \int_{t-d(t)}^{t} \mathrm{e}^{2\beta(t-s)} r^*(s) Q_{1ij} r(s)\,\mathrm{d}s, \\ V_{3ij}\big(r(t)\big) &= d \int_{-d}^{0} \int_{t+\theta}^{t} \mathrm{e}^{2\beta(t-s)} \dot{r}^*(s) Q_{2ij} \dot{r}(s)\,\mathrm{d}s\,\mathrm{d}\theta, \\ V_{4ij}\big(r(t)\big) &= \tau \int_{-\tau}^{0} \int_{t+\theta}^{t} \mathrm{e}^{2\beta(t-s)} g^*\big(r(s)\big) Q_{3ij} g\big(r(s)\big)\,\mathrm{d}s\,\mathrm{d}\theta, \\ V_{5ij}\big(r(t)\big) &= (t_{k+1} - t) \int_{t_k}^{t} \mathrm{e}^{2\beta(t-s)} \dot{r}^*(s) S_{ij} \dot{r}(s)\,\mathrm{d}s.\end{aligned}$$

After switching, system (24) is activated. We can get

$$\begin{aligned}0 = {} & \big[\dot{r}(t) + r(t_k)\big]^* G_i \big(-\dot{r}(t) - A_j r(t) + B_j g\big(r(t)\big) + C_j g\big(r\big(t - d(t)\big)\big)\big) \\ & + \big[\dot{r}(t) + r(t_k)\big]^* G_i \left(D_j \int_{t-\tau(t)}^{t} g\big(r(s)\big)\,\mathrm{d}s + K_i r(t_k) \right) \\ & + \big(-\dot{r}(t) - A_j r(t) + B_j g\big(r(t)\big) + C_j g\big(r\big(t - d(t)\big)\big)\big)^* G_i^* \big[\dot{r}(t) + r(t_k)\big] \\ & + \left(D_j \int_{t-\tau(t)}^{t} g\big(r(s)\big)\,\mathrm{d}s + K_i r(t_k) \right)^* G_i^* \big[\dot{r}(t) + r(t_k)\big].\end{aligned}$$

Similarly, we have

$$\dot{V}_{ij}\big(r(t)\big) \leqslant 2\beta V_{ij}\big(r(t)\big) + \Phi^*(t) \Xi_{ij} \Phi(t),$$

it is obvious that

$$\dot{V}_{ij}\big(r(t)\big) < 2\beta V_{ij}\big(r(t)\big). \tag{26}$$

Integrating inequality (26) yields

$$V_{ij}\big(r(t)\big) < \mathrm{e}^{2\beta(t-t_k-\bar{t})}V_{ij}\big(r(t_k+\bar{t})\big). \tag{27}$$

Since the construct of LKF (11), (25), and (8), we can obtain

$$V_{ij}\big(r(t_k+\bar{t})\big) \leqslant \mu V_i\big(r(t_k+\bar{t})^-\big), \qquad V_j\big(r(t_{k+1})\big) \leqslant \mu V_{ij}(t_{k+1}^-). \tag{28}$$

For all $t \in [t_k, t_{k+1}]$, combining Lemma 2 with (22), (23), and (27)–(28), we have

$$\begin{aligned} V_{\sigma(t)}\big(r(t)\big) &\leqslant \mu^{2N_\sigma(t_0,t)}\mathrm{e}^{2(\alpha+\beta)N_\sigma(t_0,t)h_k}\mathrm{e}^{-2\alpha(t-t_0)}V_{\sigma(t_0)}(t_0) \\ &\leqslant \mathrm{e}^{2((\alpha+\beta)h_k+\ln\mu)(N_0+(t-t_0)/\tau_a)}\mathrm{e}^{-2\alpha(t-t_0)}V_{\sigma(t_0)}(t_0) \\ &\leqslant \mathrm{e}^{2((\alpha+\beta)h_k+\ln\mu)N_0}\mathrm{e}^{2(((\alpha+\beta)h_k+\ln\mu)/\tau_a-\alpha)(t-t_0)}V_{\sigma(t_0)}(t_0). \end{aligned}$$

Defining $c = \mathrm{e}^{2((\alpha+\beta)h_k+\ln\mu)N_0}$, $\lambda = 2(\alpha - ((\alpha+\beta)h_k + \ln\mu)/\tau_a) > 0$, the ADT τ_a is restricted through (9). Then

$$V_{\sigma(t)}\big(r(t)\big) < c\mathrm{e}^{-2\lambda(t-t_0)}V_{\sigma(t_0)}\big(r(t_0)\big).$$

Based on the LKF candidate, scalars a and b satisfy

$$a\big\|r(t)\big\|^2 \leqslant V_{\sigma(t)}\big(r(t)\big), \qquad V_{\sigma(t_0)}\big(r(t_0)\big) \leqslant b\big\|r(t_0)\big\|^2.$$

Thus, the following inequality can be derived:

$$\big\|r(t)\big\|^2 \leqslant \frac{1}{a}V_{\sigma(t)}\big(r(t)\big) \leqslant \frac{b}{a}c\mathrm{e}^{-2\lambda(t-t_0)}\big\|r(t_0)\big\|^2.$$

According to Definition 1, for any switching signal satisfying ADT (9), system (5) with asynchronous switching is exponentially stable. □

Remark 1. The designed Lyapunov functional involving sampling intervals is combined with (17) to transform nonlinear or coupling terms into optimizable matrix forms. Compared with the traditional continuous free-weight matrix method, the discrete sampling-point free-weight matrix method can more effectively reduce the conservativeness of stability criteria.

Remark 2. The sampled-data controller in 1 ensures the exponential stability of system (5) under asynchronous switching. While existing literature (e.g., [3, 7]) does not address asynchronous switching (prevalent in practice), this paper investigates such phenomena in QVSNNs, inspired by [10].

Remark 3. Case 1: controller and system always match, converging exponentially with decay rate α. Case 2: controller and system match before switching; after switching, the controller remains unchanged in the sampling interval, and their mismatch may cause instability. Our control strategy allows the system to diverge at rate β.

Next, we consider the system free of asynchronous phenomena, i.e., switching occurs only at sampling instants with the controller and system always matched. Corollary 1 presents a stability criterion for switched QVSNNs without asynchronous switching and derives the corresponding ADT.

Corollary 1. *Under Assumptions* 1–2*, suppose that for $\alpha > 0$ and any μ, there exist positive definite Hermitian matrices $P_i, Q_{1i}, Q_{2i}, Q_{3i}, S_i, L_i, R_{1i}, R_{2i} \in \mathbb{R}^{n\times n}$ and any matrices M_i, G_i, guaranteeing the feasibility of the LMIs*

$$\Xi_i = \begin{bmatrix} \Xi_{11i} & -A_i^*G_i^* & 0 & 0 & P_i^*B_i & P_i^*C_i & 0 & P_i^*D_i & \Xi_{19i} \\ * & \Xi_{22i} & 0 & 0 & G_iB_i & G_iC_i & 0 & G_iD_i & M_i - G_i^* \\ * & * & \Xi_{33i} & 0 & 0 & 0 & 0 & 0 & 0 \\ * & * & * & \Xi_{44i} & 0 & 0 & 0 & 0 & 0 \\ * & * & * & * & \Xi_{55i} & 0 & 0 & 0 & B_i^*G_i^* \\ * & * & * & * & * & \Xi_{66i} & 0 & 0 & C_i^*G_i^* \\ * & * & * & * & * & * & \Xi_{77i} & 0 & 0 \\ * & * & * & * & * & * & * & \Xi_{88i} & D_i^*G_i^* \\ * & * & * & * & * & * & * & * & \Xi_{99i} \end{bmatrix} \prec 0,$$

where

$$\begin{aligned} \Xi_{11i} &= 2\alpha P_i - A_i^*P_i - P_i^*A_i + Q_{1i} + L_i^*R_{1i}L_i - \frac{1}{h}\mathrm{e}^{-2\alpha h}S_i - \mathrm{e}^{2\alpha d}Q_{2i}, \\ \Xi_{19i} &= \frac{1}{h}\mathrm{e}^{-2\alpha h}S_i + P_iG_i^{-1}M_i - A_i^*G_i^*, \qquad \Xi_{22i} = d^2Q_{2i} + hS_i - G_i - G_i^*, \\ \Xi_{33i} &= -(1-d_1)\mathrm{e}^{-2\alpha d}Q_{1i} + L_i^*R_{2i}L_i, \qquad \Xi_{44i} = -\mathrm{e}^{2\alpha d}Q_{2i}, \\ \Xi_{55i} &= \tau^2Q_{3i} - R_{1i}, \qquad \Xi_{66i} = -R_{2i}, \qquad \Xi_{77i} = -\mathrm{e}^{2\alpha d}\frac{1}{d}Q_{2i}, \\ \Xi_{88i} &= -\mathrm{e}^{2\alpha\tau}Q_{3i}, \qquad \Xi_{99i} = -\frac{1}{h}\mathrm{e}^{-2\alpha h}S_i + M_i + M_i^*, \\ Q_{1j} &= \mu Q_{1i}, \qquad Q_{2j} = \mu Q_{2i}, \qquad Q_{3j} = \mu Q_{3i}, \\ P_j &= \mu P_i, \qquad S_j = \mu S_i. \end{aligned} \tag{29}$$

Then the ADT satisfies

$$\tau_a \geqslant \frac{\ln\mu}{2\alpha}. \tag{30}$$

Proof. As in Case 1 of Theorem 1, the system and controller are matched. We can construct the LKF candidate similar to (11). The following inequality holds:

$$\dot{V}_i\big(r(t)\big) < -2\alpha V_i\big(r(t)\big). \tag{31}$$

For all $t \in [t_k, t$, integrating (31) yields

$$V_i\big(r(t)\big) < \mathrm{e}^{-2\alpha(t-t_k)} V\big(r(t_k)\big). \tag{32}$$

From Definition 2, (29), and (32) we can obtain

$$\begin{aligned} V_{\sigma(t)}\big(r(t)\big) &\leqslant \mu \mathrm{e}^{-2\alpha(t-t_k^-)} V_{\sigma(t_k^-)}\big(r(t_k^-)\big) \\ &\leqslant \mathrm{e}^{N_\sigma(t_0,t) ln\mu} \mathrm{e}^{-2\alpha(t-t_0)} V_{\sigma(t_0)}\big(r(t_0)\big) \\ &\leqslant \mathrm{e}^{(N_0+t/\tau_a) ln\mu} \mathrm{e}^{-2\alpha(t-t_0)} V_{\sigma(t_0)}\big(r(t_0)\big). \end{aligned}$$

By defining $c = N_0 ln\mu$, $\lambda = 2\alpha - \ln \mu/\tau_a$, we have

$$V_{\sigma(t)}\big(r(t)\big) < c\mathrm{e}^{-2\lambda(t-t_0)} V_{\sigma(t_0)}\big(r(t_0)\big).$$

Based on the LKF candidate, scalars a and b satisfy

$$a\big\|r(t)\big\|^2 \leqslant V_{\sigma(t)}\big(r(t)\big), \qquad V_{\sigma(t_0)}\big(r(t_0)\big) \leqslant b\big\|r(t_0)\big\|^2.$$

Thus, it can be obtained

$$\big\|r(t)\big\|^2 \leqslant \frac{1}{a} V_{\sigma(t)}\big(r(t)\big) \leqslant \frac{b}{a} c\mathrm{e}^{-2\lambda(t-t_0)} \big\|r(t_0)\big\|^2.$$

Finally, for any switching signal satisfying ADT (30), the error system (5) with no asynchronous phenomenon is exponentially stable. □

We now consider the following exponential synchronization of the QVNN without switches. Thus, the system (5) is simplified as

$$\begin{aligned} \dot{r}(t) = &-Ar(t) + Bg\big(r(t)\big) + Cg\big(r\big(t - d(t)\big)\big) \\ &+ D \int_{t-\tau(t)}^{t} g\big(r(s)\big)\,\mathrm{d}s + Kr(t_k). \end{aligned} \tag{33}$$

Corollary 2. *For a constant $\alpha > 0$, let there exist positive definite Hermitian matrices P, Q_1, Q_2, Q_3, L, $R_1, R_2 \in \mathbb{R}^{n\times n}$ and any matrices M, G guaranteeing the feasibility of the LMIs*

$$\Xi = \begin{bmatrix} \Xi_{11} & -A^*G^* & 0 & 0 & P^*B & P^*C & 0 & P^*D & \Xi_{19} \\ * & \Xi_{22} & 0 & 0 & GB & GC & 0 & GD & M - G^* \\ * & * & \Xi_{33} & 0 & 0 & 0 & 0 & 0 & 0 \\ * & * & * & \Xi_{44} & 0 & 0 & 0 & 0 & 0 \\ * & * & * & * & \Xi_{55} & 0 & 0 & 0 & B^*G^* \\ * & * & * & * & * & \Xi_{66} & 0 & 0 & C^*G^* \\ * & * & * & * & * & * & \Xi_{77} & 0 & 0 \\ * & * & * & * & * & * & * & \Xi_{88} & D^*G^* \\ * & * & * & * & * & * & * & * & \Xi_{99} \end{bmatrix} \prec 0, \tag{34}$$

where

$$\Xi_{11} = 2\alpha P - A^*P - P^*A + Q_1 + L^*R_1L - \frac{1}{h}\mathrm{e}^{-2\alpha h}S - \mathrm{e}^{2\alpha d}Q_{2i},$$
$$\Xi_{19} = \frac{1}{h}\mathrm{e}^{-2\alpha h}S + PG^{-1}M - A^*G^*, \qquad \Xi_{22} = d^2Q_2 + hS - G - G^*,$$
$$\Xi_{33} = -(1-d_1)\mathrm{e}^{-2\alpha d}Q_1 + L^*R_2L, \qquad \Xi_{44} = -\mathrm{e}^{2\alpha d}Q_2,$$
$$\Xi_{55} = \tau^2Q_3 - R_1, \qquad \Xi_{66} = -R_2, \Xi_{77} = -\mathrm{e}^{2\alpha d}\frac{1}{d}Q_2,$$
$$\Xi_{88} = -\mathrm{e}^{2\alpha\tau}Q_3, \qquad \Xi_{99} = -\frac{1}{h}\mathrm{e}^{-2\alpha h}S + M + M^*.$$

Then the error system (33) *can be exponentially stable through the controller given by* $K = G^{-1}M$ *when the decay rate* α *is properly set. The following inequality is obtained:*

$$\big\|r(t)\big\| \leqslant \sqrt{\frac{b}{a}}\mathrm{e}^{-2\alpha(t-t_0)}\big\|r(t_0)\big\|.$$

Remark 4. Obviously, if there is only one subsystem, conditions (34) are satisfied, which can be simplified by Theorem 1. The presented method can be applied to system (33) through simplification resulting in Corollary 2. In other words, the problem solved in this paper generalizes the existing ones in [23]. The corollaries in this literature can also be easily derived from this paper.

4 Numerical example

The effectiveness and practical applicability of the proposed method are demonstrated by two comprehensive numerical examples.

Example 1. Firstly, we choose system (33) as an example, where the parameters are

$$A = \begin{bmatrix} 0.35 & 0 \\ 0 & 0.35 \end{bmatrix},$$
$$B = \begin{bmatrix} 0.295+0.0141\mathrm{i}+0.055\mathrm{j}+0.0098\mathrm{k} & 0.0072+0.001\mathrm{i}-0.0095\mathrm{j}+0.0048\mathrm{k} \\ 0.0086+0.001\mathrm{i}+0.005\mathrm{j}+0.039\mathrm{k} & 0.395+0.0097\mathrm{i}+0.017\mathrm{j}+0.026\mathrm{k} \end{bmatrix},$$
$$C = \begin{bmatrix} -0.808+0.0058\mathrm{i}+0.0012\mathrm{j}+0.0021\mathrm{k} & 0.026+0.003\mathrm{i}+0.0054\mathrm{j}-0.0038\mathrm{k} \\ -0.037+0.022\mathrm{i}+0.0035\mathrm{j}+0.0189\mathrm{k} & -0.817+0.016\mathrm{i}-0.0146\mathrm{j}+0.0084\mathrm{k} \end{bmatrix},$$
$$D = \begin{bmatrix} -0.2055+0.006\mathrm{i}+0.0032\mathrm{j}+0.001\mathrm{k} & 0.0079-0.0014\mathrm{i}+0.0031\mathrm{j}+0.001\mathrm{k} \\ 0.0096+0.005\mathrm{i}+0.0093\mathrm{j}+0.001 & -0.2598+0.005\mathrm{i}+0.0076\mathrm{j}+0.001\mathrm{k} \end{bmatrix}.$$

The remaining parameters of the system: $g(r(t)) = 1.4\tanh(r(t)$, $d(t) = \mathrm{e}^t/(1+\mathrm{e}^t)$, $\tau(t) = 0.55 + 0.5\sin^2 t$, $d = 1$, $\tau = 0.85$, $d_1 = 0.5$, $\alpha = 0.8$, $h = 0.09$, $L = \left[\begin{smallmatrix} 1 & 0 \\ 0 & 1 \end{smallmatrix}\right]$.

Table 1. Control gain corresponding to different sampling moments h.

k				
$h = 0.01$	$h = 0.03$	$h = 0.05$	$h = 0.07$	$h = 0.09$
$\begin{bmatrix} 0.9938 & -0.0120 \\ -0.0122 & 0.9502 \end{bmatrix}$	$\begin{bmatrix} 1.0312 & -0.0120 \\ -0.0121 & 0.9877 \end{bmatrix}$	$\begin{bmatrix} 1.0005 & -0.0124 \\ -0.0125 & 0.9554 \end{bmatrix}$	$\begin{bmatrix} 0.9207 & -0.0132 \\ -0.0133 & 0.8721 \end{bmatrix}$	$\begin{bmatrix} 1.2908 & -0.0141 \\ -0.0141 & 1.2180 \end{bmatrix}$

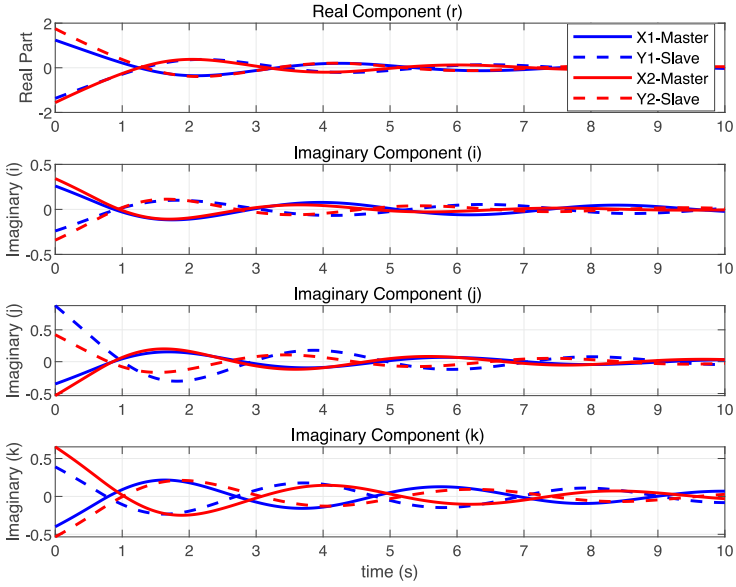

Figure 1. The response curve of uncontrolled QVNNs.

With LMI, we can obtain the gain matrix K for different sampling moments h (see Table 1).

Set initial states

$$x(t) = \begin{bmatrix} 1.24 + 0.26\mathrm{i} - 0.35\mathrm{j} - 0.4\mathrm{k} \\ -1.56 + 0.342\mathrm{i} - 0.533\mathrm{j} + 0.654\mathrm{k} \end{bmatrix},$$

$$y(t) = \begin{bmatrix} -1.37 - 0.24\mathrm{i} + 0.88\mathrm{j} + 0.39\mathrm{k} \\ 1.75 - 0.342\mathrm{i} + 0.423\mathrm{j} - 0.534\mathrm{k} \end{bmatrix}.$$

The response curve of uncontrolled QVNNs is first exhibited in Fig. 1, which shows that the state trajectories of master-slave systems are different. From Table 1, when $h = 0.09$, the controller gain is given as follows:

$$K = \begin{bmatrix} 1.2908 & -0.0141 \\ -0.0141 & 1.2180 \end{bmatrix}.$$

Applying Corollary 2 to inequality (34) and using the MATLAB toolbox yields a feasible solution at the maximum sampling moment. The trend of the state variables of system (33) over time is shown in Figs. 1–2.

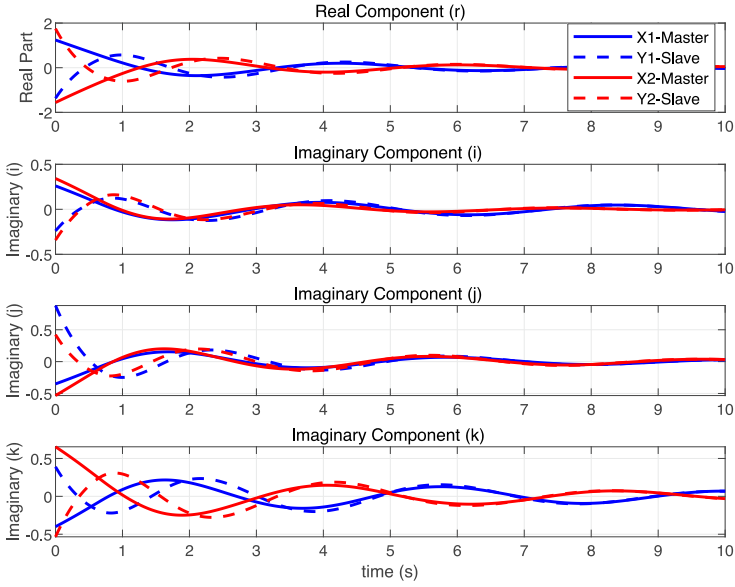

Figure 2. The response curve of controlled QVNNs.

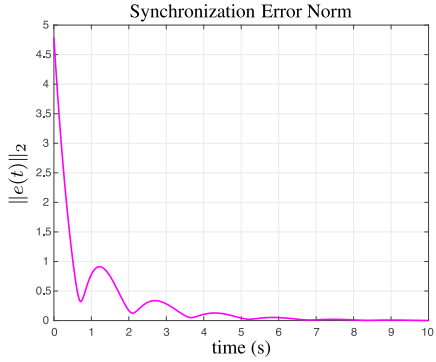

Figure 3. The response curve of error system.

Remark 5. As shown in Fig. 3, the eventual zero-convergence of state variables confirms that the above nonswitching method is applicable to QVNNs for exponential master-slave synchronization, thereby validating its feasibility.

Example 2. Consider system (5) in Theorem 1 with two subsystems. The parameters are:

$$A_1 = \begin{bmatrix} 0.45 & 0 \\ 0 & 0.45 \end{bmatrix}, \qquad A_2 = \begin{bmatrix} 0.55 & 0 \\ 0 & 0.55 \end{bmatrix},$$

$$B_1 = B_2 = \begin{bmatrix} 0.295 + 0.14\mathrm{i} + 0.55\mathrm{j} + 0.98\mathrm{k} & 0.72 + 0.176\mathrm{i} - 0.95\mathrm{j} + 0.48\mathrm{k} \\ 0.86 + 0.341\mathrm{i} + 0.568\mathrm{j} + 0.39\mathrm{k} & 0.395 + 0.097\mathrm{i} + 0.247\mathrm{j} + 0.26\mathrm{k} \end{bmatrix},$$

$$C_1 = C_2 = \begin{bmatrix} -0.3 + 0.5\mathrm{i} + 0.3\mathrm{j} + 0.6\mathrm{k} & 0.8 + 0.8\mathrm{i} + 0.15\mathrm{j} - 0.1\mathrm{k} \\ -0.3 + 0.5\mathrm{i} + 0.8\mathrm{j} + 0.5\mathrm{k} & -0.3 + 0.5\mathrm{i} - 0.3\mathrm{j} + 0.25\mathrm{k} \end{bmatrix},$$

$$D_1 = D_2 = \begin{bmatrix} -0.255 + 0.6\mathrm{i} + 0.32\mathrm{j} + 0.104\mathrm{k} & 0.9 - 0.14\mathrm{i} + 0.31\mathrm{j} + 0.671\mathrm{k} \\ 0.6 + 0.5\mathrm{i} + 0.93\mathrm{j} + 0.253\mathrm{k} & -0.2598 + 0.5\mathrm{i} + 0.76\mathrm{j} + 0.1\mathrm{k} \end{bmatrix}.$$

The remaining parameters of the system: $g(r(t)) = 0.155\tanh(r(t))$, $d(t) = \mathrm{e}^t/(1+\mathrm{e}^t)$, $\tau(t) = 0.55 + 0.5\sin^2 t$, $L_i = L_j = \left[\begin{smallmatrix} 1 & 0 \\ 0 & 1 \end{smallmatrix}\right]$, $d = 0.8$, $\tau = 0.4$, $d_1 = 0.35$, $\alpha = 0.4$, $\beta = 1$, $\mu = 0.9$.

With LMIs, we can obtain the gain matrix K for different sampling moments h (see Table 2). From Table 2, when $h = 0.09$, the controller gain is given as follows:

$$K = \begin{bmatrix} 0.3271 & -0.4127 \\ -0.4090 & 0.5206 \end{bmatrix}.$$

From (9) the minimum mean residence time can be obtained as τ_a^* = 0.2266. Let the switching sequence be defined to satisfy $\tau_a > \tau_a^*$. The initial condition is set as

$$x(t) = \begin{bmatrix} 0.524 - 0.483\mathrm{i} + 0.548\mathrm{j} - 0.449\mathrm{k} \\ -0.156 + 0.342i - 0.533j + 0.654k \end{bmatrix},$$

$$y(t) = \begin{bmatrix} -0.482 + 0.574\mathrm{i} - 0.498\mathrm{j} + 0.554\mathrm{k}, \\ 0.175 - 0.342\mathrm{i} + 0.423\mathrm{j} - 0.534\mathrm{k} \end{bmatrix}.$$

The system's state variables' time curve is presented in Figs. 4 and 5.

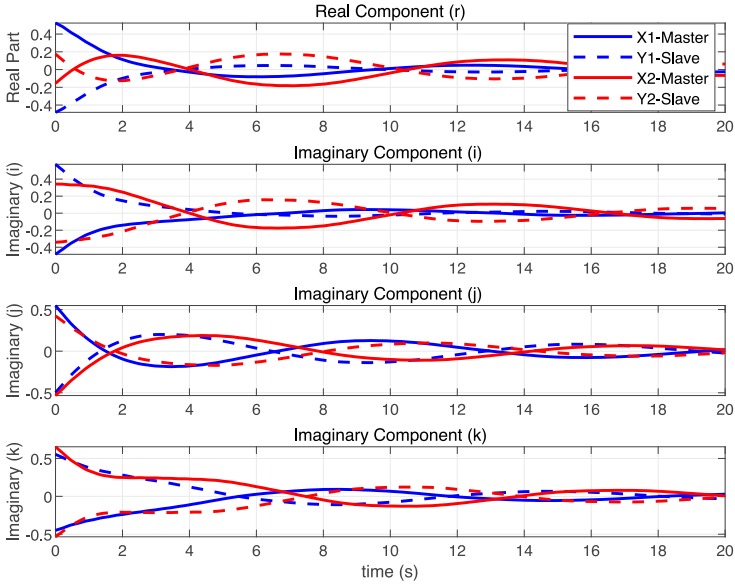

Figure 4. The response curve of uncontrolled QVSNNs.

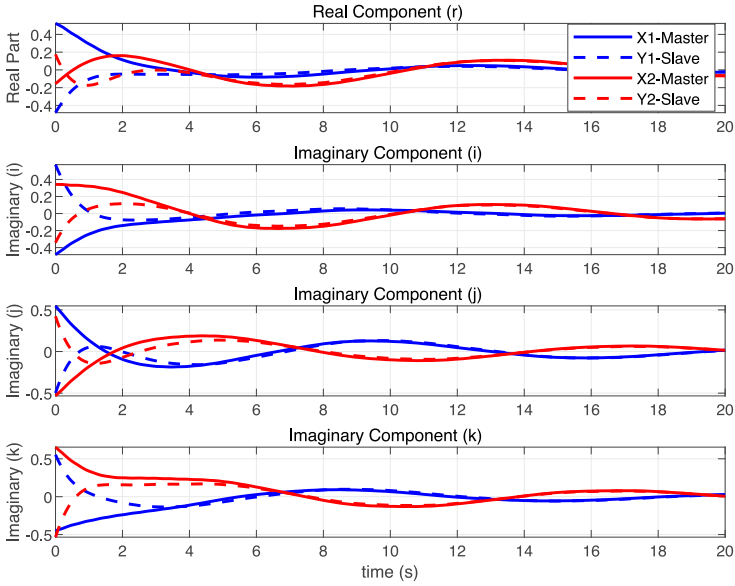

Figure 5. The response curve of controlled QVSNNs.

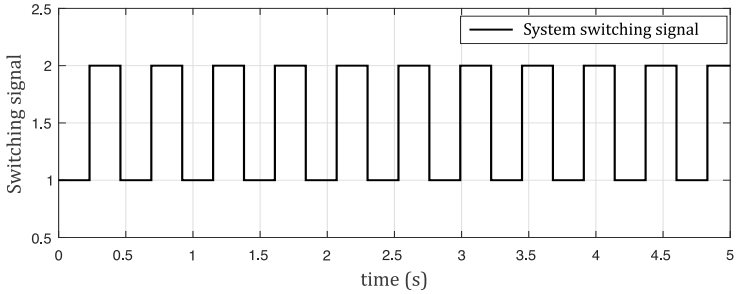

Figure 6. Switching sequence diagrams.

Table 2. Control gain corresponding to different sampling moments h.

k				
$h = 0.01$	$h = 0.04$	$h = 0.07$	$h = 0.1$	$h = 0.14$
$\begin{bmatrix} 1.2627 & -0.6730 \\ -0.6645 & 1.3930 \end{bmatrix}$	$\begin{bmatrix} 1.1837 & -0.7128 \\ -0.7018 & 1.3155 \end{bmatrix}$	$\begin{bmatrix} 0.9768 & -0.8630 \\ -0.8441 & 1.1127 \end{bmatrix}$	$\begin{bmatrix} 0.8370 & -0.8703 \\ -0.8689 & 1.0486 \end{bmatrix}$	$\begin{bmatrix} 0.3271 & -0.4127 \\ -0.4090 & 0.5206 \end{bmatrix}$

Remark 6. As shown in Fig. 6, from the resulting data we know that the sampling signal of the system always lags behind the switching signal. With the sampled-data control input, the QVSNNs can be synchronized in an exponential manner. The purpose of this example is to show that the method of designing an asynchronous switching controller for system (5) is effective and feasible.

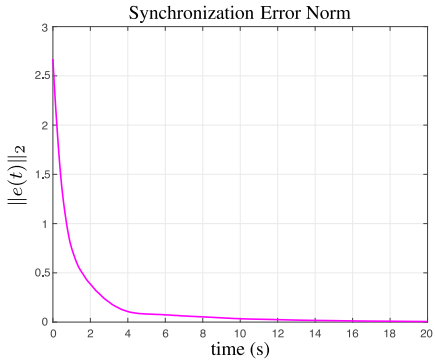

Figure 7. The response curve of error system.

5 Conclusion

This paper explores exponential synchronization of QVSNNs with mixed delays via state-feedback-dependent control (with asynchronous switching considered). It derives ADT sampling interval links, uses Lyapunov functions and integral inequalities to design a low-conservatism controller, and gives sufficient synchronization conditions (numerically verified). Future work will extend to QVSNNs with PID controllers for networked control systems.

Author contributions. All authors (W.T., Y.Z., T.P., Z.T., and Y.D.) have contributed as follows: conceptualization, W.T. and Y.Z.; methodology, W.T.; validation, W.T., Z.T., and T.P.; formal analysis, Y.D. and Y.Z.; investigation, Y.Z.; resources, Y.Z., T.P., and Z.T.; data curation, W.T. and Y.D.; writing – original draft, W.T.; writing – review & editing, W.T. Z.T., and T.P.; visualization, W.T.; supervision, Y.Z.; project administration, Z.T. and T.P.; funding acquisition, Y.Z., T.P., and Z.T. All authors have read and approved the published version of the manuscript.

Conflicts of interest. The authors declare no conflicts of interest.

Acknowledgment. First and foremost, the authors would like to sincerely acknowledge the referee for their thorough comments and insightful suggestions, which have greatly improved the quality of this article.

References

1. L. Deckers, L. Van Damme, W. Van Leekwijck, I.J. Tsang, S. Latré, Co-learning synaptic delays, weights and adaptation in spiking neural networks, *Front. Neurosci.*, **18**:1360300, 2024, https://doi.org/10.3389/fnins.2024.1360300.
2. C. Ge, J.H. Park, C. Hua, C. Shi, Robust passivity analysis for uncertain neural networks with discrete and distributed time-varying delays, *Neurocomputing*, **364**:330–337, 2019, https://doi.org/10.1016/j.neucom.2019.06.077.

3. Y. Han, J. Lian, Synchronization of switched neural networks with time-varying delays via sampled-data control, *Asian J. Control*, **21**:1260–1269, 2019, https://doi.org/10.1002/asjc.1803.
4. Q. Huang, Y. Yu, J. Cao, Projective synchronization of inertial quaternion-valued neural networks via non-reduced order approach, *Neural Process. Lett.*, **56**:21, 2024, https://doi.org/10.1007/s11063-024-11523-1.
5. Y. Ji, X. Liu, Unified synchronization criteria for hybrid switching-impulsive dynamical networks, *Circ. Syst. Signal Process.*, **34**:1499–1517, 2015, https://doi.org/10.1007/s00034-014-9916-0.
6. B. Jiang, J. Lou, J. Lu, K. Shi, Synchronization of chaotic neural networks: Average-delay impulsive control, *IEEE Trans. Neural Netw. Learn. Syst.*, **33**:6007–6012, 2021, https://doi.org/10.1109/TNNLS.2021.3069830.
7. X. Li, R. Wang, B. Yang, W. Wang, Stability analysis for delayed neural networks via some switching methods, *IEEE Trans. Syst. Man Cybern. Syst.*, **50**:1690–1695, 2018, https://doi.org/10.1109/TSMC.2017.2782233.
8. Y. Li, B. Li, S. Yao, L. Xiong, The global exponential pseudo almost periodic synchronization of quaternion-valued cellular neural networks with time-varying delays, *Neurocomputing*, **303**:75–87, 2018, https://doi.org/10.1016/j.neucom.2018.04.044.
9. Z. Li, F. Cheng, J. Tang, H. Dong, J. Tang, Synchronization for stochastic switched networks via delay feedback control, *Complex Eng. Syst.*, **4**, 2024, https://doi.org/10.20517/ces.2024.14.
10. J. Lian, C. Li, B. Xia, Sampled-data control of switched linear systems with application to an F-18 aircraft, *IEEE Trans. Ind. Electron.*, **64**:1332–1340, 2016, https://doi.org/10.1109/TIE.2016.2618872.
11. Y. Liu, D. Zhang, J. Lou, J. Lu, J. Cao, Stability analysis of quaternion-valued neural networks: Decomposition and direct approaches, *IEEE Trans. Neural Netw. Learn. Syst.*, **29**:4201–4211, 2018, https://doi.org/10.1109/TNNLS.2017.2755697.
12. Q. Ouyang, Z. Wu, Y. Cong, Z. Wang, Formation control of unmanned aerial vehicle swarms: A comprehensive review, *Asian J. Control*, **25**:570–593, 2023, https://doi.org/10.1002/asjc.2806.
13. T. Peng, J. Qiu, J. Lu, Z. Tu, J. Cao, Finite-time and fixed-time synchronization of quaternion-valued neural networks with/without mixed delays: An improved one-norm method, *IEEE Trans. Neural Netw. Learn. Syst.*, **33**:7475–7487, 2021, https://doi.org/10.1109/TNNLS.2021.3085253.
14. T. Peng, Y. Wu, Z. Tu, A.S. Alofi, J. Lu, Fixed-time and prescribed-time synchronization of quaternion-valued neural networks: A control strategy involving lyapunov functions, *Neural Netw.*, **160**:108–121, 2023, https://doi.org/10.1016/j.neunet.2022.12.014.
15. Y. Qi, X. Zhao, J. Fu, P. Zeng, W. Yu, Event-triggered control for switched systems under multiasynchronous switching, *IEEE Trans. Syst. Man Cybern. Syst.*, **52**:4685–4696, 2021, https://doi.org/10.1109/TSMC.2021.3102406.
16. S. Singh, U. Kumar, S. Das, F. Alsaadi, J. Cao, Synchronization of quaternion valued neural networks with mixed time delays using lyapunov function method, *Neural Process. Lett.*, **54**:785–801, 2022, https://doi.org/10.1007/s11063-021-10657-w.

17. Q. Song, Y. Chen, Z. Zhao, Y. Liu, F.E. Alsaadi, Robust stability of fractional-order quaternion-valued neural networks with neutral delays and parameter uncertainties, *Neurocomputing*, **420**: 70–81, 2021, https://doi.org/10.1016/j.neucom.2020.08.059.
18. Q. Song, Q. Wu, Y. Liu, Stabilization of chaotic quaternion-valued neutral-type neural networks via sampled-data control with two-sided looped functional approach, *Nonlinear Anal. Model. Control*, **29**(6):1150–1166, 2024, https://doi.org/10.15388/namc.2024.29.37852.
19. R. Sriraman, O. Kwon, Global exponential synchronization of delayed quaternion-valued neural networks via decomposition and non-decomposition methods and its application to image encryption, *Mathematics*, **12**:33–45, 2024, https://doi.org/10.3390/math12213345.
20. Z. Tu, X. Yang, L. Wang, N. Ding, Stability and stabilization of quaternion-valued neural networks with uncertain time-delayed impulses: Direct quaternion method, *Physica A*, **535**: 122358, 2019, https://doi.org/10.1016/j.physa.2019.122358.
21. Z. Wang, H. Wu, X. Wang, Sampled-data control for linear time-delay distributed parameter systems, *ISA Trans.*, **92**:75–83, 2019, https://doi.org/10.1016/j.isatra.2019.02.002.
22. Y. Wu, Z. Tu, N. Dai, L. Wang, N. Hu, T. Peng, Stability analysis of quaternion-valued neutral neural networks with generalized activation functions, *Cogn. Comput.*, **16**:392–403, 2024, https://doi.org/10.1007/s12559-023-10212-w.
23. Z. Wu, P. Shi, H. Su, J. Chu, Exponential synchronization of neural networks with discrete and distributed delays under time-varying sampling, *IEEE Trans. Neural Netw. Learn. Syst.*, **23**: 1368–1376, 2012, https://doi.org/10.1109/TNNLS.2012.2202687.
24. K. Xiong, C. Hu, J. Yu, Direct approach-based synchronization of fully quaternion-valued neural networks with inertial term and time-varying delay, *Chaos Solitons Fractals*, **172**: 113556, 2023, https://doi.org/10.1016/j.chaos.2023.113556.
25. L. Yang, W. Ma, X. Wang, Lagrange stability and passivity in the mean square sense of discrete-time stochastic Markovian switched neural networks with time-varying mixed delays, *Appl. Math. Comput.*, **477**:128800, 2024, https://doi.org/10.1016/j.amc.2024.128800.
26. X. Yang, X. Wan, Z. Cheng, J. Cao, Y. Liu, L. Rutkowski, Synchronization of switched discrete-time neural networks via quantized output control with actuator fault, *IEEE Trans. Neural Netw. Learn. Syst.*, **32**:4191–4201, 2021, https://doi.org/10.1109/TNNLS.2020.3017171.
27. D. Zhang, X. Liao, B. Yang, Y. Zhang, A fast and efficient approach to color-image encryption based on compressive sensing and fractional fourier transform, *Multimedia Tools Appl.*, **77**: 2191–2208, 2018, https://doi.org/10.1007/s11042-017-4370-1.
28. H. Zhang, Y. Zhao, L. Xiong, J. Dai, Y. Zhang, New event-triggered synchronization criteria for fractional-order complex-valued neural networks with additive time-varying delays, *Fractal Fract.*, **8**, 2024, https://doi.org/10.3390/fractalfract8100569.
29. L. Zhang, R. Wei, J. Cao, X. Ding, Synchronization control of quaternion-valued inertial memristor-based neural networks via adaptive method, *Math. Methods Appl. Sci.*, **47**:581–599, 2024, https://doi.org/10.1002/mma.10936.
30. W. Zhao, Y. Sun, Absolute exponential stability of switching time-delay lurie systems with the application to switching hopfield neural networks, *Nonlinear Anal. Model. Control*, **30**(1):40–57, 2025, https://doi.org/10.15388/namc.2025.30.38317.